Design and Simulation of Integral Twist Control for Helicopter Vibration Reduction

Sangjoon Shin, Carlos E. S. Cesnik, and Steven R. Hall

Abstract: Closed-loop active twist control of integral helicopter rotor blades is investigated in this paper for reducing hub vibration induced in forward flight. A four-bladed fully articulated integral twist-actuated rotor system has been designed and tested successfully in wind tunnel in open-loop actuation. The integral twist deformation of the blades is generated using active fiber composite actuators embedded in the composite blade construction. An analytical framework is developed to examine integrally twisted helicopter blades and their aeroelastic behavior during different flight conditions. This aeroelastic model stems from a three-dimensional electroelastic beam formulation with geometrical-exactness, and is coupled with finite-state dynamic inflow aerodynamics. A system identification methodology that assumes a linear periodic system is adopted to estimate the harmonic transfer function of the rotor system. A vibration minimizing controller is designed based on this result, which implements a classical disturbance rejection algorithm with some modifications. Using the established analytical framework, the closed-loop controller is numerically simulated and the hub vibratory load reduction capability is demonstrated.

Keywords: Closed-loop control design and simulation, helicopter vibration, integral twist-actuated rotor blade, linear time-periodic system.

1. INTRODUCTION

There have been considerable efforts in the helicopter community to reduce fuselage vibration, which is mainly induced by an asymmetric distribution of the unsteady aerodynamic loads acting on the blades. Most of those were based on passive methodologies [1]. However, during the last two decades, active methods to alleviate helicopter vibration based on the idea of directly modifying unsteady aerodynamic loads acting upon the rotor blades have been studied. These may be broadly classified as higher harmonic control (HHC) and individual blade control (IBC) [2,3]. Several outstanding results were obtained that showed vibration reduction. Examples include analytical studies searching for an optimal control scheme [4], wind tunnel tests with either small or full-scaled model [2,5], and flight tests [6]. However, these realizations, associated with employing additional hydraulic actuators installed on either non-rotating (beneath swashplate) or rotating frames (between pitch links), have not successfully entered into full-scale application. Typical disadvantages were identified, such as adverse power requirement and limitation on excitation frequency in HHC, and extreme mechanical complexity of hydraulic sliprings in IBC.

Recently, advances in active materials have enabled multiple lightweight sensors/actuators embedded or surface-mounted at several locations in rotor blades [7-9]. By employing active materials for such actuators, one can potentially obtain advantages in terms of weight and power consumption when compared with traditional hydraulic systems. Various implementations have been suggested for active materials application to reduce vibration in rotorcraft [10].

Among those implementations, the integral twist actuation concept [11-14] is the selected mechanism for blade control in the present study. This actuation

Sangjoon Shin is with the School of Mechanical and Aerospace Engineering and the Institute of Advanced Aerospace Technology, Seoul National University, 56-1 Shillim-dong, Kwanak-gu, Seoul 151-744, Korea (e-mail: ssjoon@snu.ac.kr).

Carlos E. S. Cesnik is with the Department of Aerospace Engineering, University of Michigan, 1320 Beal Ave., Ann Arbor, MI 48109, U.S.A. (e-mail: cesnik@umich.edu).

Steven R. Hall is with the Department of Aeronautics and Astronautics, Massachusetts Institute of Technology, 77 Massachusetts Ave., Cambridge, MA 02139, U.S.A. (e-mail: srhall@mit.edu).

concept presents itself as an aggressive alternative with several potential benefits. Besides providing redundancy in operation, the integral concept does not increase the profile drag of the blade like discrete flap concepts. Moreover, the actuators once embedded in the composite construction become part of the load bearing structure, making the active blade a truly integrated multifunctional structure that allows for effective construction and assembly of future low vibration rotor blades.

The integral twist actuation concept using active materials technology has shown promising benefits from a conceptual standpoint [15], as well as from hover testing with small-scaled models [13, 16]. The research activities which have been conducted so far under the present research are described in detail in the relevant references: structural modeling of the integral blades [17]; blade design, prototyping, and its bench test [14]; hover test and its correlation with analysis [16,18]; open-loop forward flight test and its correlation with analysis [19,20]; and the closed-loop control experiment under the forward flight [21].

This paper focuses on the system identification and closed-loop control of active twist rotors. It also illustrates the analytical framework for simulating the forward flight response of the helicopter rotor system employing active composite blades with distributed anisotropic piezoelectric strain actuators. An active blade is analyzed in a two-step approach as follows. First, its cross section is modeled as a multi-cell composite beam with integral anisotropic actuators [22,23]. Then, its result is added to a multi-body dynamics model of the rotor [24], which combines a geometrically-exact beam structural analysis and a finite-state dynamic inflow theory for aerodynamics [27]. Using the forward flight analysis, system identification is conducted to estimate the harmonic transfer functions of the active rotor system [26,27]. From that, linear time-periodic (LTP) components of these transfer functions are extracted in addition to linear time-invariant (LTI) ones. Since the helicopter rotor becomes a LTP system during forward flight due to a periodicity in aerodynamics, these LTP components exist and may potentially impact the closed-loop response. Based on the system identification results, a vibration minimizing closed-loop controller is designed. It implements a classical disturbance rejection algorithm [28]. Stability of the closed-loop system is examined prior to applying the controller, and phase and gain modification is added to it as necessary. Numerical simulation of the resultant closed-loop controller is conducted using the proposed analytical framework.

The specific objectives of this paper are:
1. Establish an aeroelastic framework to simulate active twist rotor systems.
2. Identify the harmonic transfer functions of the

active rotor during forward flight based on LTP system approach.
3. Design a vibration minimizing closed-loop controller for the active rotor and numerically simulate its capability.

2. ANALYTICAL FRAMEWORK

For analyzing helicopter blades with embedded strain actuators, a framework is needed such that the effects of the active material embedded in the structure are carried out throughout all the steps of the analysis. Since there were no analysis formulations available which could properly handle all the peculiarities of an active helicopter blade cross section, the authors have created a general framework for active rotor blade modeling. Here, an asymptotical analysis takes the electromechanical three-dimensional problem and reduces it into a set of two analyses: a linear analysis over the cross section and a nonlinear analysis of the resulting beam reference line. By coupling the active blade formulation with the appropriate unsteady aerodynamics, the aeroelastic problem can then be solved in time and simulations be conducted for control design. A schematic diagram of the established framework is shown in Fig. 1.

2.1. Cross-sectional analysis

Stiffness and actuation forcing constants for an active anisotropic thin-walled two-cell beam are obtained from a variational asymptotic formulation [17]. While restricted to thin-walled beams, it yields closed form solutions of the displacement field (which is derived and not assumed), and stiffness and
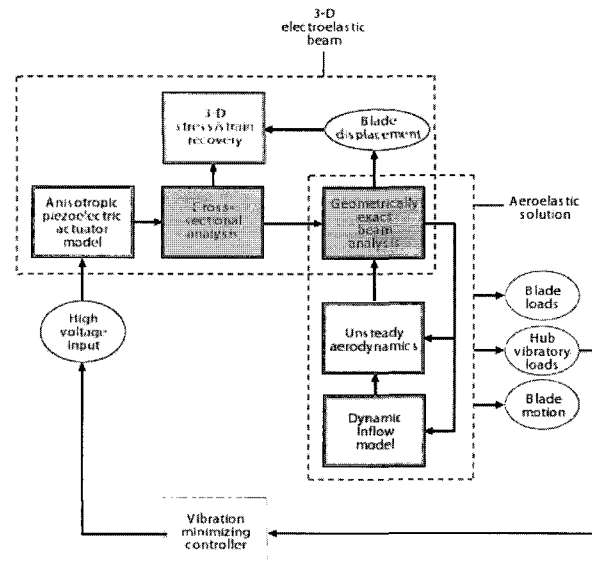

Fig. 1. Schematic diagram of the analytical framework for an active helicopter blade and its aeroelastic behavior.

actuation constants. The availability of closed form expressions was essential to determine design paradigms on this new type of blade, mainly concerning the tradeoffs between torsional stiffness and twist actuation. A more general active cross sectional analysis compatible with this framework and capable of handling thin and thick walls, even solid arbitrary-shape cross sections was developed by Cesnik and Ortega-Morales [22], and later extended by Palacios and Cesnik [23]. These stiffness and actuation constants are then used in the beam finite element discretization of the blade reference line.

2.2. Beam structure and aerodynamic analyses

To simulate the active rotor system for open and closed-loop control, a time domain formulation is needed. The multi-body dynamics code DYMORE, developed by Bauchau and co-workers [24], is based on the geometrically-exact beam equations and it is coupled to the aerodynamics of Peters and He [25]. DYMORE's original beam formulation is consistent with the one used previously by the authors in studying hover response of the active rotor system. The difference now is that the formulation is displacement-based instead of mixed-form. Therefore, the same cross-sectional analysis for active beams can be used. The integral actuation forces and moments existing inside the blade structure are realized in the form of finite element loads to the passive beam in the modified time domain analysis. The solution of the 1-D beam analysis provides blade displacement and generalized stress fields due to external loading and piezoelectric actuation, which are of interest in the analysis of static and dynamic deformations and aeroelastic stability.

To simulate the active twist rotor system, a time domain formulation is needed. The multi-body dynamics code DYMORE, developed by Bauchau and co-workers [24], is based on the geometrically-exact beam equations and it is coupled to the aerodynamics of Peters and He [25]. DYMORE's original beam formulation is consistent with the one used previously by the authors in investigating the hover response of the active rotor system. The difference is that the DYMORE's formulation is a displacement-based form instead of the mixed-form. Therefore, the cross-sectional analysis developed by the authors for active beams is incorporated in DYMORE in this paper. The integral actuation forces and moments existing inside the blade structure are realized in the form of finite element loads to the passive beam in the presently modified new version of DYMORE. In what follows, the modifications to the existing formulations of DYMORE for the present active beam analysis are briefly described.

The kinetic and strain energies of the beam are expressed as follows.

$$K = \frac{1}{2}\int_0^L \begin{Bmatrix} V_B \\ \Omega_B \end{Bmatrix}^T \begin{Bmatrix} P_B \\ H_B \end{Bmatrix} dx_1,$$

$$U = \frac{1}{2}\int_0^L \begin{Bmatrix} \gamma_B \\ \kappa_B \end{Bmatrix}^T \begin{Bmatrix} F_B \\ M_B \end{Bmatrix} dx_1,$$

(1)

where K and U are the kinetic and potential energies of the blade, F_B and M_B internal force and moment column vectors, P_B and H_B linear and angular momentum column vectors, V_B and Ω_B linear and angular velocity column vectors, γ_B and κ_B the generalized strain column vectors, respectively. The quantities with the subscript B means those under the deformed blade configuration. The velocity-displacement and strain-displacement relationships are described as

$$\begin{Bmatrix} V_B \\ \Omega_B \end{Bmatrix} = \begin{bmatrix} \left(C^{ba}\right)^T \left(C^{Bb}\right)^T \dot{u} \\ \left(C^{ba}\right)^T \left(C^{Bb}\right)^T \omega \end{bmatrix},$$

$$\begin{Bmatrix} \gamma_B \\ \kappa_B \end{Bmatrix} = \begin{bmatrix} \left(C^{ba}\right)^T \left(C^{Bb}\right)^T \left(u_0' + u'\right) - 1 \\ \left(C^{ba}\right)^T \left(C^{Bb}\right)^T k \end{bmatrix},$$

(2)

where the superscripts b, B, and a mean the undeformed, deformed and the inertial blade frames of reference, and the matrices C with the appropriate superscripts are the direction cosine matrices signifying the transformation among those frames. ω is the sectional angluar velocity vector; u_0 defines the position of a point on the reference line before deformation, measured in a frame; u defines the displacement of a point to the deformed configuration, meaured in a frame; and k is the sectional elastic curvature vector. The dot means a derivative with respect to time and the prime with respective to the blade reference line x_1. The relations presented in Eq. (2) are geometrically exact, which means that they are valid for arbitrarily large displacements and rotations, although the strains are assumed to be small. The equations of motion for the blade are derived from Hamilton's principle, such as

$$\int_{t_i}^{t_f} \left[\delta\left(K + U\right) + \delta W\right] dt = 0,$$

(3)

where δW is the variation of the virtual work done by the externally applied loads, such as aerodynamic forces. By incorporating (1), one obtains

$$\int_{t_i}^{t_f} \left[\begin{Bmatrix} \delta V_B \\ \delta \Omega_B \end{Bmatrix}^T \begin{Bmatrix} P_B \\ H_B \end{Bmatrix} - \begin{Bmatrix} \delta \gamma_B \\ \delta \kappa_B \end{Bmatrix}^T \begin{Bmatrix} F_B \\ M_B \end{Bmatrix} + \delta W \right] dt = 0. (4)$$

The sectional internal forces are now substituted with the constitutive relation, which has been suggested by the authors, considering the existence of the actuation forcing vector. The sectional momenta is also represented by an appropriate inertial matrix as well. Substituting (2) into (4), and integrating by parts yield the governing simultaneous equations as follows.

$$\left(C^{Bb}C^{ba}P_B\right)^{\bullet} - \left(C^{Bb}C^{ba}F_B\right)'$$

$$= \hat{\mathbf{q}} + \left(C^{Bb}C^{ba}F_B^{(a)}\right)'\left(C^{Bb}C^{ba}H_B\right)^{\bullet}$$

$$- \tilde{\mathbf{u}}^T C^{Bb}C^{ba}P_B - \left(C^{Bb}C^{ba}M_B\right)' \qquad (5)$$

$$+ \left(\mathbf{u}_0' + \mathbf{u}'\right)^T C^{Bb}C^{ba}F_B$$

$$= \tilde{\mathbf{q}} - \left(C^{Bb}C^{ba}M_B^{(a)}\right)' + \left(\mathbf{u}_0' + \mathbf{u}'\right)^T C^{Bb}C^{ba}F_B^{(a)},$$

where $\mathbf{q}^T = \begin{bmatrix} \hat{\mathbf{q}}^T & \tilde{\mathbf{q}}^T \end{bmatrix}$ are the externally applied loads per unit span length, measured in a frame. As desribed earlier, the effect of the actuation forcing vector is treated as an additional external load in the right-hand side of (5). This is a new formulation obtained and used in the present paper to analyze the behavior of the active blades in forward flight condition. In the previous formulation obtained for the bench and hover analysis, the effect of actuation forcing vectors remained as an auxillary form to reinforce the generalized strain variables [18]. The solution of the present 1-D beam analysis provides blade displacement and generalized stress fields due to external loading and piezoelectric actuation, which are of interest in the analysis of static and dynamic deformations and aeroelastic stability.

The forward flight part of the finite-state dynamic inflow aerodynamics model [25] had already been implemented in DYMORE. This model is constructed by applying the acceleration potential theory to the rotor aerodynamics problem with a skewed cylindrical wake. More specifically, the induced flow at the rotor disk is expanded in terms of modal functions. As a result, a three-dimensional, unsteady induced-flow aerodynamics model with finite number of states is derived in time domain. This model falls on an intermediate level of wake representation between the simplest momentum and the most complicated free wake methodologies. It does not require an intense computational effort, and it is applicable to the problems of rotor aeroelastic stability, basic blade-passage vibrations, and higher-harmonic control studies [24].

2.3. Aeroelastic system in forward flight

The aeroelastic system of equations that combines the structural and aerodynamic equations obtained in the previous steps is now solved for forward flight transient response. Specifically, the present analysis adopts a direct time integration of the blade response due to integral actuation during flight. DYMORE adopts a time-discontinuous integration scheme with energy decaying characteristics in order to avoid high frequency numerical oscillation [24, 29]. Such an adverse high frequency oscillation usually occurs during a finite element time integration of a complex multi-body dynamic system. Finally, the transfer functions due to high voltage actuation input can be calculated by Fourier transform of the time response of the blade or the entire active rotor system for different forward flight conditions.

3. ROTOR CHARACTERISTICS

The basic requirements for the integral twist-actuated blade originate from an existing passive blade. The baseline (passive) system has been well studied and characterized over the years, and is representative of a generic production helicopter [30]. The active blade is designed based on the external dimensions and aerodynamic properties of the existing baseline blade to be tested in heavy gas medium. Table 1 summarizes the general dimension

Table 1. Characteristics of the active blade.

| Description	Value
Rotor type	Fully articulated
Number of blades	4
Blade chord	10.77 cm
Blade radius	1.397 m
Solidity	0.0982
Section airfoil	NACA 0012
Blade pretwist	-10°
Hinge offset	7.62 cm
Root cutout	31.75 cm
Pitch axis	25% chord
Tension axis	34.4% chord
Center of gravity	17.9% chord
Lock number	9.0
Tip Mach number	0.6
Centrifugal loading at tip	738.5 g
Rotor speed	687.5 rpm
Rotor over speed	756 rpm
EA	$1.787\ 10^1$ N
GJ	$3.143\ 10^1$ N-m^2
EI$_{\text{flap}}$	$4.419\ 10^1$ N-m^2
EI$_{\text{lag}}$	$1.153\ 10^3$ N-m^2
Sectional torsional inertia	$3.810\ 10^{-4}$ kg-m
1$^{\text{st}}$ torsional natural frequency at 100% rpm	5.97/rev
Twist actuation at 0 rpm, 2,000 V$_{\text{pp}}$/0 V$_{\text{DC}}$	2.46°/m (peak-to-peak)
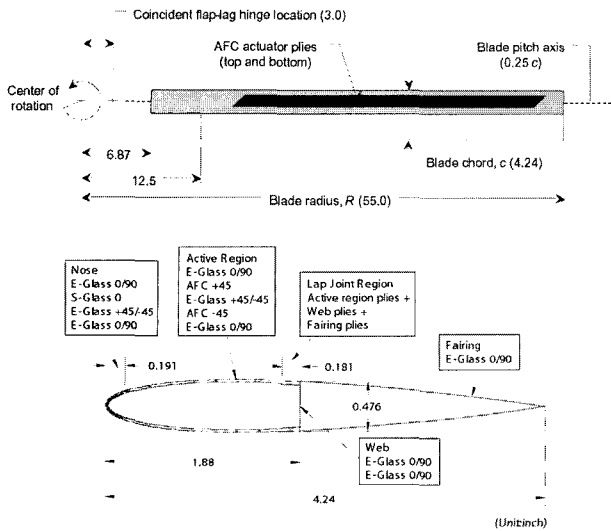
Fig. 2. Planform and cross section of the active blade (Dimensions are in inches.)
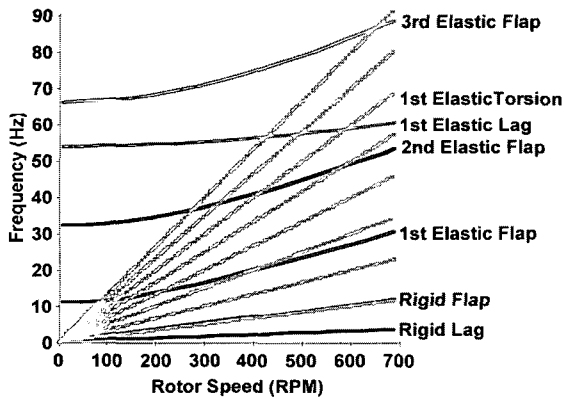
Fig. 3. Frequencies of the active blade used in the present paper.

4. NUMERICAL SYSTEM IDENTIFICATION

During forward flight, a helicopter rotor blade exhibits an aerodynamic environment that varies itself within the rotor revolution. This implies that the helicopter rotor system in forward flight is essentially a linear time-periodic system. Therefore, a methodology considering this periodicity should be used for its characterization. In this paper, a method is

adopted which results in multi-component harmonic transfer functions [31]. The theoretical background of the adopted methodology and its implementation schemes that include additional assumptions imposed on the harmonic transfer functions are described in detail in Reference [31].

Sinusoids are used to determine transfer functions, and more specifically, sine-sweep waves (chirp signals) are used to obtain the system response over a specific range of frequencies. Using the sine-sweep input signal, fixed- and rotating-system response of the active rotor system are predicted by the proposed analysis. At first, a series of collective mode actuation signal is applied, and its response is examined for the system identification. Before applying the system identification algorithm [31], the amplitude of the baseline loads must be subtracted from those under actuation. This is due to the definition of the transfer matrix that will be used in the foregoing closed-loop controller design, as represented by the following equation.

$$z = z_0 + Tu,$$ (6)
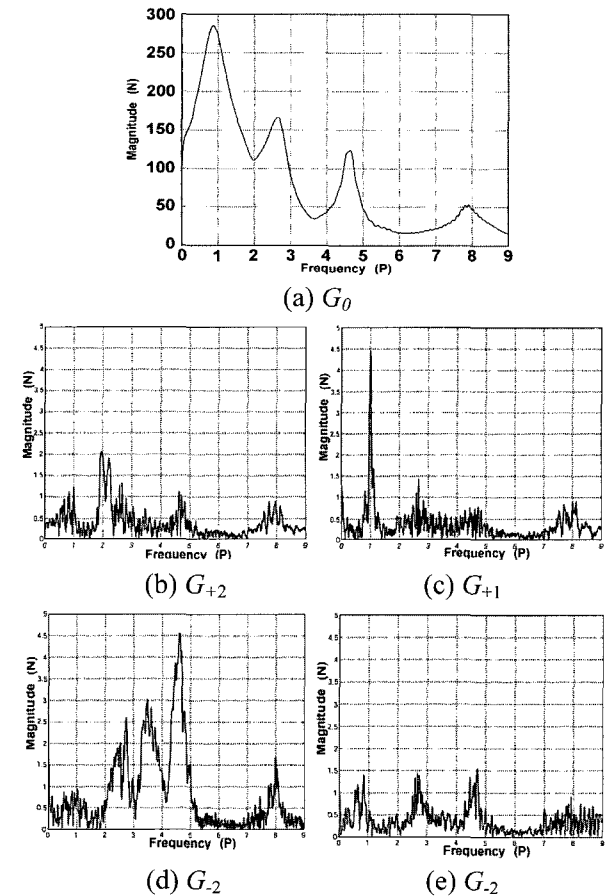
where z is a vector of vibration amplitudes, T is the

(a) G_0

(b) G_{+2} (c) G_{+1}

(d) G_{-2} (e) G_{-2}

Fig. 4. Five harmonic transfer functions estimated for the hub vertical shear loads during the collective mode actuation.
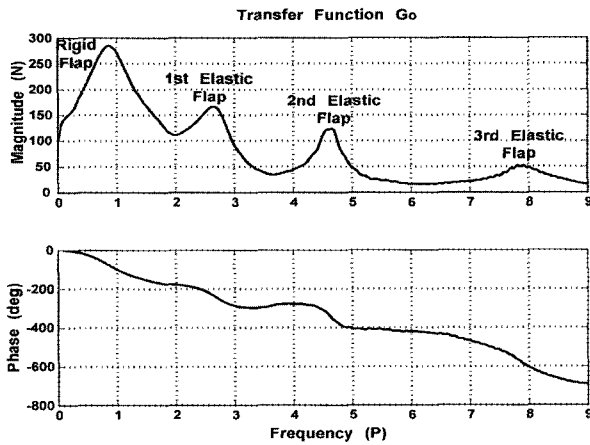
and shape characteristics of the designed active blade.

The resultant active blade employed a total of 24 active fiber composite (AFC) packs placed on the front spar only, and distributed in 6 stations along the blade span [21]. Fig. 2 shows basic blade planform and cross section characteristics selected for the present active blade. The material properties of the passive prepregs and the active fiber composite plies used in the blade are summarized in the appendices of Reference [14]. The fan plot of the active blade is plotted in Fig. 3.

Fig. 5. Harmonic transfer function G_0 of the hub vertical shear loads during the collective mode actuation.

Fig. 6. Matrix of G_0 for three components of hub shear vibratory loads versus the three modes of blade actuation.

transfer matrix, **u** is the vector of the actuation amplitudes into the AFC actuators, and z_0 is the vector of the vibration amplitudes with no actuation (baseline).

Five harmonic transfer functions, G_{-2}, G_{-1}, G_0, G_{+1}, G_{+2}, are estimated as shown in Fig. 4. These transfer function estimates are obtained by division of the power and cross spectral density functions of input (actuator voltage) and output (hub shear loads). Although the present system identification is conducted on a deterministic system, such extra consideration for an uncertainty existing in the stochastic experimental system is already included. As can be seen from these plots, G_0 has amplitude that is significantly larger compared with the others. Therefore, the higher order ones can be neglected. This indicates that the response of the active rotor system can be described only by the G_0 component, behaving like a linear time-invariant (LTI) system. More insight about the blade dynamics can be extracted from a Bode diagram of the G_0 component for the hub vertical force as shown in Fig. 5. It is recognized that the peaks approximately match the frequencies of rigid and elastic flap bending modes of the blade. (See the fan plot shown in Fig. 3.)

Sine-sweep input signals for longitudinal and lateral cyclic mode of blade actuation can be also generated. In the collective mode, all four blades have the same synchronous input signals for actuation. In the longitudinal cyclic mode, only two blades located near the longitudinal azimuth have a specified actuation while the remaining two blades with zero actuation. And, a similar actuation fashion is created for the lateral cyclic mode. By putting these input signals and executing the same identification process as described before, harmonic transfer functions corresponding to these two modes of actuation are estimated. Again, all the other components except G_0 resulted in much lower magnitudes. Therefore, the
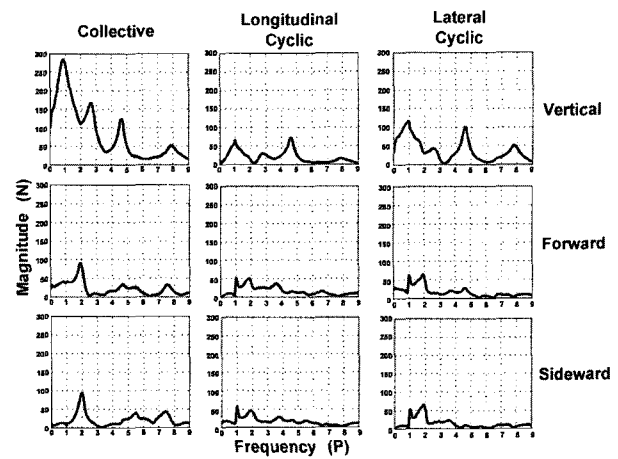
LTI simplification is still valid for these modes of actuation. All the identification results including the collective mode previously obtained may be represented as a transfer matrix relating three components of the hub shear loads versus three modes of blade actuation signal as shown in Fig. 6.

Consider the case of alleviating only the vertical components of the 4P hub shear vibratory load. From the open-loop actuation estimation presented in References [19] and [20], the baseline amplitude of this vibratory component was predicted to be approximately 23 N. However, from Fig. 6, the amplitudes associated with the hub vertical vibratory load altered by the application of each actuation mode are found to be 45 N, 26 N, and 28 N at 4P frequency, respectively. Theoretically, it can be concluded that the application of only collective mode of blade actuation is enough for a complete elimination of the 4P hub vertical vibratory load at this given flight condition. However, experimental results do not indicate this complete elimination by the collective mode only [19,20].

This contradiction results from the same discrepancy generally found in the load amplitude results predicted by the analysis and measured in the experiment, regarding the baseline loads and those under actuation. Again, for the hub vertical shear vibratory component, the 4P baseline load was predicted to be 23 N, and the amplitude under collective mode actuation was predicted to be 45 N (at 4P). However, in the experiment, the corresponding quantities for the baseline load was observed to be 90 N and the amplitude altered by the 4P IBC-mode actuation to be approximately 20 N at its maximum [19,20]. Note that the 4P IBC-mode actuation is exactly the same as the collective mode actuation at 4P. From the present discussion, few items are suggested for future study as follows. First, an

improvement on the analysis model is recommended regarding its load prediction. Second, regarding the closed-loop control for the experimental apparatus, an appropriate combination of the three modes is recommended. This multi-mode combination becomes equivalent to IBC mode, which was shown to be most effective in the open-loop control test [20]. This multi-mode controller can be configured for suppressing multi-component of hub shear vibratory loads simultaneously.

5. CLOSED-LOOP CONTROL SIMULATION

System identification results in the previous section are utilized here to design a closed-loop controller for hub shear vibratory load reduction. Under the assumption of quasi-steady condition and linearity, the amplitudes of the sine and cosine components of the vibrations at the N/rev frequency can be formulated as in (6). In that equation, z_0 is the disturbance to be rejected. The control algorithm traditionally adopted by previous researchers [2,4,6] is based on the idea of canceling the disturbance z_0 by use of the higher harmonic swashplate input u. In their traditional application, the HHC signal was applied upon the swashplate. In the present paper, it is applied into the AFC actuators in a form of an electric field. Since the disturbance z_0 is unknown, the approach is to measure the vibration at each time step and adjust the swashplate input u to just cancel that disturbance. The resulting control becomes

$$\mathbf{u}_{n+1} = \mathbf{u}_n - \mathbf{T}^{-1}\mathbf{z}_n, \tag{7}$$

where the subscripts denote the index of the time step. The measurement of the vibration z_n is accomplished by a Fourier decomposition of the vibration at the N/rev frequency. A block diagram of the resulting controller is shown in Fig. 7. This control algorithm exhibits a quite involving structure due to the modulation and demodulation tasks located in front of and behind the inverted -$\mathbf{T}$ matrix. The necessity of these modulation and demodulation tasks is originated
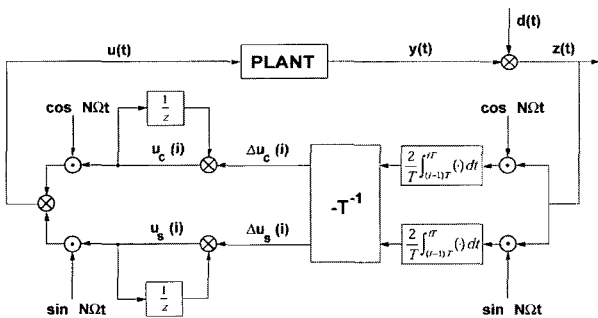

Fig. 7. Block diagram of the higher harmonic control system adopted in [2,4,6] using quasi-steady helicopter plant model.

partly from the fact that the constant control response matrix $\mathbf{T}$ is evaluated by the sine-dwell open-loop actuation at N/rev frequency. However, it was shown that such control algorithm for vibration rejection could be reduced to a simple LTI system [28]. According to this, the block diagram in Fig. 7 becomes equivalent to an LTI feedback compensation structure with the compensator, $K(s)$, as follows.

$$K(s) = \frac{2k(As + BN\Omega)}{s^2 + (N\Omega)^2}, \tag{8}$$

where

$$k = 1/T,$$

$$A = \text{Re}\left\{\frac{1}{G(jN\Omega)}\right\}, \quad B = -\text{Im}\left\{\frac{1}{G(jN\Omega)}\right\},$$

and T is the blade passage period. Furthermore, note that this LTI feedback compensation structure is essentially the same as a classical disturbance rejection algorithm, which is to eliminate an almost pure harmonic signal at constant frequency. Stability and performance issues of the closed-loop system associated with this feedback compensator are discussed in Reference [28]. Note also that the $\mathbf{T}$ matrix is constructed using the previous system identification result, which reflects an uncertainty existing in the system. However, for implementation of the present controller in the stochastic experimental setup, additional consideration needs to be included for an uncertainty existing in instrumentation of the reference signal. For example, an anti-windup scheme may be added to the present control design to prevent an unrealistic control signal, which results from noise in measurement.

Before implementing the controller, the stability of the closed-loop system should be examined. For this purpose, a loop gain, which is a product of the identified plant transfer function, $G_0(s)$, and the designed compensator, $K(s)$, is investigated in frequency domain. Among the transfer matrix components presented in Fig. 5, the one for the hub vertical shear related only with the collective mode actuation is considered first. This implies a single-input single-output controller that suppresses the hub vertical vibratory loads by only using the collective mode of blade actuation. Its capability of complete vibration elimination within the hub vertical loads is already predicted in the previous section. The Nichols plot of the present closed-loop system without any modification applied to $K(s)$ is represented with dashed lines in Fig. 8. The stability of the system is ensured if there are no encirclements of the critical point (unity magnitude at 180° of phase). In the same plot, contours of constant disturbance attenuation (or amplification) are also shown. Along the loop gain
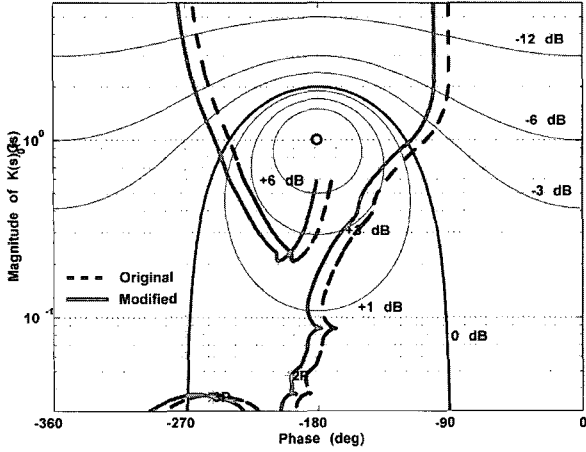
Fig. 8. Nichols plot of the loop transfer function, original and modified.

line, corresponding frequencies are marked with asterisks to see which frequency content is involved with a possible instability near the critical point. According to Fig. 8, the present controller with the unmodified $K(s)$ has gain margin of approximately 5.4 dB (indicated as the downward arrow in the figure), and phase margin of 90°. If the gain of the controller is increased, the closed-loop gain line is shifted upward, and the gain margin is diminished. A modification on the original controller is possible to increase the gain margin, and therefore, the controller performance while maintaining stability. This is accomplished by shifting the closed-loop gain by 13°. The new loop transfer function is shown in Fig. 8 by the solid line. This shift increases the gain margin by extra 2 dB and reduces the phase margin to 80°. Another modification to (8) is the addition of a pole at 0.4P. This is done so that the controller does not alter the steady state component of the thrust by rolling off its gain at low frequencies. Therefore, the final form for the controller transfer function $K(s)$ becomes

$$K(s) = \frac{s}{(s + N\Omega/10)} \frac{2k(As + BN\Omega)}{\left[s^2 + (N\Omega)^2 \right]} e^{j(13°)}. \quad (9)$$

So far, only one component among the transfer functions, $G_0(s)$, has been used to represent the plant for the stability check and preliminary performance estimation. This simplification is due to the previous finding that more than 90% of the system response can be represented with $G_0(s)$ only under the three modes of blade actuation. In the following simulation, however, the complete helicopter model will be combined with the resulting controller for its demonstration.

The resulting LTI feedback controller can be easily incorporated in the analytical framework established previously by transforming it into a discrete-time
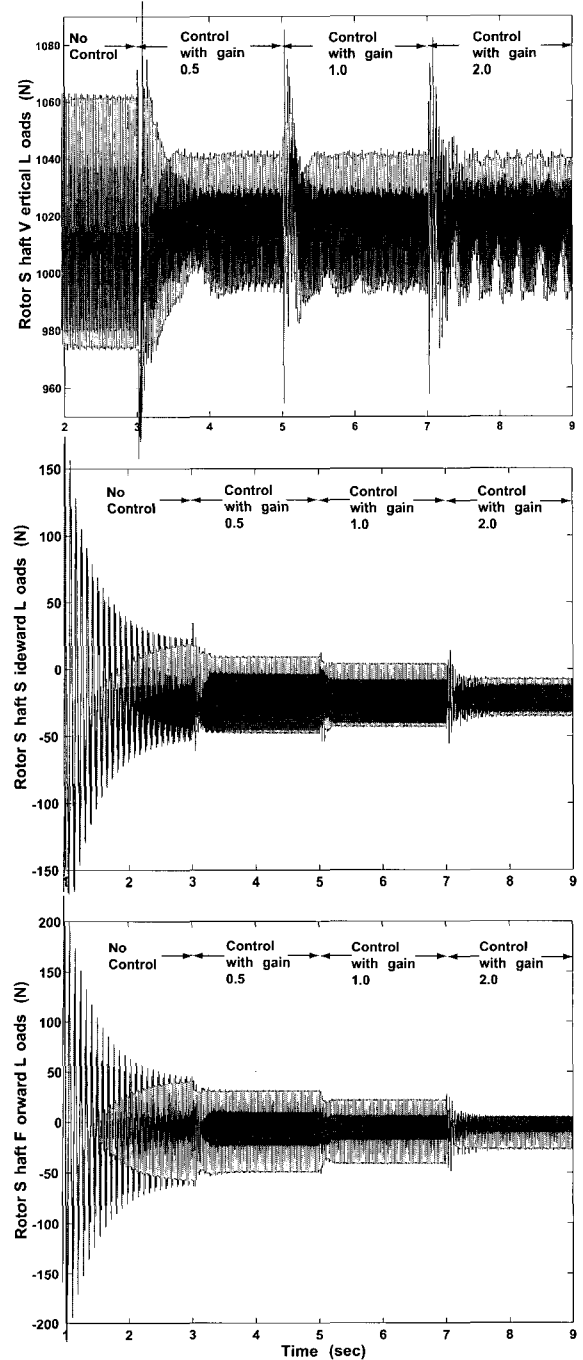

Fig. 9. Time history of the hub shear loads for μ = 0.333, α_S = -6°, C_T = 0.0066 without and with the closed-loop controller engaged: vertical, sideward, and forward load components.

state-space approximation. It is still required to establish a steady-state equilibrium for a specific flight condition before engaging the controller. Otherwise, large hub vibratory loads, which are induced during the transient period before the steady state equilibrium is reached, may generate unrealistically large control signal. Then, the controller is engaged with a different gain constants discretely adjusted at 0.5, 1.0, and 2.0 within each 2-

second period. The result of the present simulation is plotted as a time history of the three components for the hub shear loads in Fig. 9. The vibratory load components without control action are significantly reduced by the controller engagement. By adjusting the controller gain in the controller, different response behaviors are obtained. By increasing the gain, the settling time for the response is improved. However, all the different gains seem to produce a similar degree of vibration reduction by qualitatively examining the time response. This suggests a closer investigation of the power spectral density distribution of the hub vertical loads in frequency domain. The results for the vertical hub shear load with and without the controller engaged are shown in Fig. 10. The vibratory load component at 4P is decreased by different degree for each gain constant applied, and more than 90% of the 4P vibratory load in the original response is removed with the controller on. However, outside the narrow band of 4P frequency, undesirable amplification is induced by the controller. Also, significant vibration is found at integral multiples of 4P (e.g., amplitude at 8P in Fig. 10). These vibration components are rarely affected by the current controller design, and explain the remnant vibration after the 4P component is removed. Therefore, it is recommended to augment the present 4P controller into parallel ones targeted at multiple harmonic components [32] in order to reduce other vibration components simultaneously. Frequency spectrum analysis of the generated control signal reveals that it is mainly composed of 3P sinusoidal signals, as shown in Fig. 11. The large 3P component in it is a result of the combination of the collective and cyclic modes applied at 4P. It is also observed that each blade exhibits 90^0 phase difference of its phase angle at 3P. This suggests that the 3P component of the generated
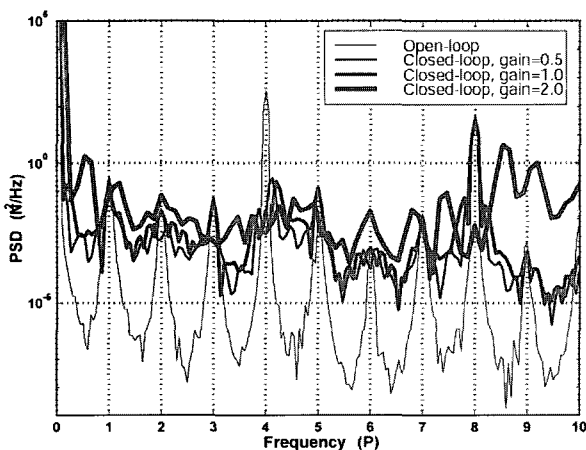

Fig. 11. Frequency spectrum of the generated blade control signals for $\mu = 0.333$, $\alpha_S = -6°$, $C_T = 0.0066$.

control signal is close to the 3P IBC actuation signal used in the open-loop control simulation and experiment [19,20]. Note again that the 3P IBC signals showed the biggest impact on the fixed-system load variation during the open-loop control test.

6. CONCLUSIONS

This paper addresses helicopter vibration reduction using integral blade twist control. A numerical aeroelastic framework is proposed for this study. For its implementation, an existing multi-body dynamics code, DYMORE, is modified to account for the distributed anisotropic piezocomposite actuators. Using the proposed analysis, system identification on the active rotor system is numerically performed. It is found that the linear time-periodic system can be represented by a linear time-invariant system under the three modes of blade actuation: collective, longitudinal cyclic, and lateral cyclic. Collective mode of actuation is found theoretically to have potential of eliminating 4P hub vibratory loads completely. This capability is demonstrated from the numerical simulation of the closed-loop controller, which is based on a classical disturbance rejection algorithm. The combination of the three modes of actuation is recommended for future closed-loop control implementations. Also, multi-harmonic controller is recommended to suppress the vibratory components at other frequencies.

Fig. 10. Power spectral density distribution of the vertical hub shear loads for $\mu = 0.333$, $\alpha_S = -6°$, $C_T = 0.0066$ without and with the closed-loop controller engaged.

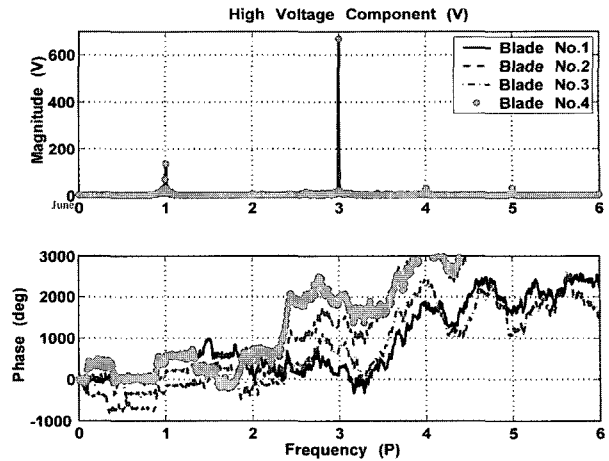## REFERENCES

[1]   R. Bielawa, Rotary Wing Structural Dynamics and Aeroelasticity, AIAA Education Series, American Institute of Aeronautics and Astronautics, 1992.

[2]   J. Shaw, N. Albion, E. J. Hanker, and R. S. Teal, "Higher harmonic control: Wind tunnel

demonstration of fully effective vibratory hub force suppression," *Journal of the American Helicopter Society*, vol. 31, no. 1, pp. 14-25, 1989.

[3] N. D. Ham, "Helicopter individual-blade-control research at MIT 1977-1985," *Vertica*, vol. 11, no. 1/2, pp. 109-122, 1987.

[4] J. A. Molusis, C. E. Hammond, and J. H. Cline, "A Unified approach to the optimal design of adaptive and gain scheduled controllers to achieve minimum helicopter rotor vibration," *Journal of the American Helicopter Society*, vol. 28, no. 2, pp. 9-18, 1983.

[5] K. Nguyen, M. Betzina, and C. Kitaplioglu, "Full-scale demonstration of higher harmonic control for noise and vibration reduction on the XV-15 rotor," *American Helicopter Society 56th Annual Forum*, Virginia Beach, VA, May 2000.

[6] E. R. Wood, R. W. Powers, J. H. Cline, and C. E. Hammond, "On developing and flight testing a higher harmonic control system," *Journal of the American Helicopter Society*, vol. 30, no. 1, pp. 3-20, 1985.

[7] R. Loewy, "Recent developments in smart structures with aeronautical applications," *Smart Materials and Structures*, vol. 6, pp. 11-42, 1997.

[8] P. P. Friedmann, "The promise of adaptive materials for alleviating aeroelastic problems and some concerns," *Innovation in Rotorcraft Technology*, London, United Kingdom, 24-25 June 1997.

[9] I. Chopra, "Status of application of smart structures technologies to rotorcraft systems," *Journal of the American Helicopter Society*, vol. 45, no. 4, pp. 228-252, 2000.

[10] V. Giurgiutiu, "Recent advances in smart material rotor control actuation," *Proc. of AIAA/ASME/ASCE/AHS/ASC41st Structures, Structural Dynamics and Materials Conference*, AIAA Paper No. 2000-1709, Atlanta, GA, April 2000.

[11] P. Chen and I. Chopra, "A feasibility study to build a smart rotor: Induced strain actuation of airfoil twisting using piezoceramic crystals," *Proc. of SPIE Smart Structures and Materials Conference*, vol. 1917, Part 1, pp. 238-254, 1993.

[12] P. Chen and I. Chopra, "Hover testing of smart rotor with induced-strain actuation of blade twist," *AIAA Journal*, vol. 35, no.1, pp. 6-16, 1997.

[13] J. P. Rodgers, and N. W. Hagood, "Preliminary mach-scale hover testing of an integral twist-actuated rotor blade," *Proc. of SPIE's 5th Annual International Symposium on Smart Structures and Materials*, San Diego, California, March 1998.

[14] C. E. S. Cesnik, S. J. Shin, W. K. Wilkie, M. L. Wilbur, and P. H. Mirick, "Modeling, design,

and testing of the NASA/Army/MIT active twist rotor prototype blade," *American Helicopter Society 55th Annual Forum*, Montreal, Canada, May 1999.

[15] R. Derham and N. Hagood, "Rotor design using smart materials to actively twist blades," *Proc. of American Helicopter Society 52nd Annual Forum*, vol. 2, pp. 1242-1252, Washington, D.C., June 1996.

[16] M. L. Wilbur, W. T. Yeager, Jr., W. K. Wilkie, C. E. S. Cesnik, and S. J. Shin, "Hover testing of the NASA/Army/MIT active twist rotor prototype blade," *American Helicopter Society 56th Annual Forum*, Virginia Beach, VA, May 2000.

[17] C. E. S. Cesnik and S. J. Shin, "On the modeling of integrally actuated helicopter blades," *International Journal of Solids and Structures*, vol. 38, no. 10-13, pp. 1765-1789, 2001.

[18] C. E. S. Cesnik, S. J. Shin, and M. L. Wilbur, "Dynamic response of active twist rotor blades," *Smart Materials and Structures - Special Issue on Rotorcraft Application*, vol. 10, pp. 62-76, 2001.

[19] S. J. Shin and C. E. S. Cesnik, "Forward flight response of the active twist rotor for helicopter vibration reduction," *Proc. of AIAA/ASME/ASCE/AHS/ ASC 42nd Structures, Structural Dynamics and Materials Conference*, AIAA Paper No. 2001-1357, Seattle, WA, April 2001.

[20] M. L. Wilbur, P. H. Mirick, W. T. Yeager, Jr., C. W. Langston, C. E. S. Cesnik, and S. J. Shin, "Vibratory loads reduction testing of the NASA/Army/MIT active twist rotor," *American Helicopter Society 57th Annual Forum*, Washington, DC, May 2001.

[21] S. J. Shin, C. E. S. Cesnik, and S. R. Hall, "Closed-loop control test of the NASA/Army/ MIT active twist rotor for vibration reduction," *Journal of the American Helicopter Society*, vol. 50, no. 2, pp. 178-194, 2005.

[22] C. E. S. Cesnik, and M. Ortega-Morales, "Active beam cross-sectional modeling," *Journal of Intelligent Material Systems and Structures*, vol. 12, no. 7, pp. 483-496, 2001.

[23] R. Palacios and C. E. S. Cesnik, "Cross-sectonal analysis of non-homogeneous anisotrpic active slender structures," *AIAA Journal*, vol. 43, no.12, pp. 2624-2638, 2005.

[24] O. A. Bauchau, "Computational schemes for flexible, nonlinear multi-body systems," *Multi-body Dynamics*, vol. 2, pp.169-225, 1998.

[25] D. A. Peters and C. J. He, "Finite state induced flow models part II: Three-dimensional rotor disk," *Journal of Aircraft*, vol. 32, no. 2, pp. 323-333, 1995.

[26] N. M. Wereley and S. R. Hall, "Linear time

periodic systems: Transfer functions, poles, transmission zeros and directional properties," *Proc. of American Control Conference*, Boston, MA, June 1991.

[27] F. Nitzsche, "Laplace-domain approximation to the transfer functions of a rotor blade in forward flight," *Aeronautical Journal*, vol. 105, no. 1077, pp. 233-240, 2001.

[28] S. R. Hall and N. M. Wereley, "Performance of higher harmonic control algorithms for helicopter vibration reduction," *Journal of Guidance, Control, and Dynamics*, vol. 16, no. 4, pp. 793-797, 1993.

[29] O. A. Bauchau and Y. G. Nikishkov, "Stability analysis of comprehensive rotorcraft models," *American Helicopter Society 56th Annual Forum*, Virginia Beach, VA, May 2000.

[30] W. K. Wilkie, M. L. Wilbur, P. H. Mirick, C. E. S. Cesnik, and S. J. Shin, "Aeroelastic analysis of the NASA/Army/MIT active twist rotor," *American Helicopter Society 55th Annual Forum*, Montreal, Canada, May 25-27, 1999.

[31] A. Siddiqi and S. R. Hall, "Identification of the harmonic transfer functions of a helicopter rotor," *AMSL Report #01-01, Active Materials and Structures Laboratory*, Massachusetts Institute of Technology, March 2001.

[32] E. F. Prechtl and S. R. Hall, "Closed-loop vibration control experiments on a rotor with blade-mounted actuation," *Proc. of AIAA/ASME/ASCE/AHS/ASC 41st Structures, Structural Dynamics and Materials Conference*, Atlanta, GA, April 2000.
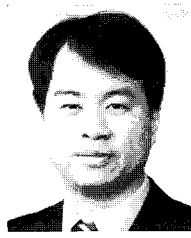
Sangjoon Shin received the S.M. and Ph.D. degrees in Aeronautics and Astronautics from Massachusetts Institute of Technology in 1999 and 2001, respectively. His research interests include aeroelasticty, rotorcraft dynamics, and smart structures.

Carlos E. S. Cesnik received the M.S. and Ph.D. degrees in Aerospace Engineering from the Georgia Institute of Technology in 1991 and 1994, respectively. His research interests include active aeroelastic structures, vibration and noise reduction in rotorcraft, and rotor modeling.
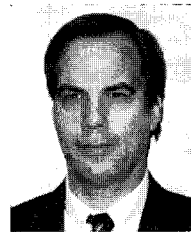
Steven R. Hall received the S.M. and Sc.D. degrees in Aeronautics and Astronautics from Massachusetts Institute of Technology in 1982 and 1985, respectively. His research interests include control of flexible structures and control of helicopter dynamics.